



## Self-discharge characteristic and mechanism of single-phase $\text{PuNi}_3$ -, $\text{Gd}_2\text{Co}_7$ -, and $\text{Pr}_5\text{Co}_{19}$ -type Nd–Mg–Ni-based alloys

Zeru Jia<sup>b,1</sup>, Lu Zhang<sup>a,1</sup>, Yumeng Zhao<sup>b</sup>, Juan Cao<sup>b</sup>, Yuan Li<sup>b</sup>, Zhentao Dong<sup>b</sup>, Wenfeng Wang<sup>b</sup>, Shumin Han<sup>a,b,\*</sup>

<sup>a</sup> State Key Laboratory of Metastable Materials Science and Technology, Yanshan University, Qinhuangdao 066004, PR China

<sup>b</sup> College of Environmental and Chemical Engineering, Yanshan University, Qinhuangdao 066004, PR China

### HIGHLIGHTS

- Single-phase  $\text{PuNi}_3$ -,  $\text{Gd}_2\text{Co}_7$ -, and  $\text{Pr}_5\text{Co}_{19}$ -type Nd–Mg–Ni alloys have been obtained.
- Self-discharge rate increases with higher  $[\text{NdNi}_5]/[\text{NdMgNi}_4]$  subunit ratio.
- Hydride stability elevates, leading to less reversible self-discharge.
- Oxidation/corrosion alleviates, leading to less irreversible self-discharge.
- Reversible self-discharge is main factor leading to self-discharge of alloys.

### ARTICLE INFO

#### Keywords:

Nickel metal hydride battery  
Self-discharge characteristic  
Nd–Mg–Ni-based alloy  
Superlattice structure  
Electrochemical property

### ABSTRACT

To decrease the self-discharge rate of the nickel metal hydride batteries, the self-discharge characteristic and mechanism of single-phase  $\text{PuNi}_3$ -,  $\text{Gd}_2\text{Co}_7$ -, and  $\text{Pr}_5\text{Co}_{19}$ -type Nd–Mg–Ni-based alloys are studied from the perspective of structure in this work. It is found that the self-discharge rate of the alloy electrodes gradually increases with a rising  $[\text{NdNi}_5]/[\text{NdMgNi}_4]$  subunit ratio. The factors resulting in reversible and irreversible self-discharge are analyzed by electrochemical pressure-composition isotherms, Tafel and SEM measurements. Electrochemical *P-C* isotherms show that with the increasing  $[\text{NdNi}_5]/[\text{NdMgNi}_4]$  subunit ratio, the hydrogen desorption plateau pressure sharply elevates, leading to less stability of the corresponding hydride and more reversible self-discharge of the alloys; whereas, corrosion current density of the three alloy electrodes gradually decreases and SEM shows that the amount of hydroxide accumulating on the alloy surface diminishes, indicating the oxidation/corrosion degree alleviates and less irreversible self-discharge with the higher  $[\text{NdNi}_5]/[\text{NdMgNi}_4]$  ratio. By calculating the proportion of reversible and irreversible self-discharge in total capacity loss, we find that the reversible self-discharge is nearly more than 90% for the three single-phase alloys, while irreversible self-discharge is less than 10%, which illustrates that reversible self-discharge is the dominate factor in self-discharge of Nd–Mg–Ni-based alloys in this study.

### 1. Introduction

Nickel metal hydride (Ni/MH) secondary batteries with high energy density, good resistance to overcharge/discharge and superior safety features have been widely applied in the market of hybrid electric vehicles, electric power tools, portable electronic devices and so on [1]. However, it suffers from high self-discharge rate, which is unsatisfactory for further industrial application. Generally, the performance of negative electrode materials is one of the main factors that

determine the self-discharge characteristic of the Ni/MH batteries. And compared with the commercialized  $\text{AB}_5$ -type alloys, rare earth (RE)–Mg–Ni-based hydrogen storage alloys, used as a new type negative electrode material of the Ni/MH batteries, not only have the advantages of higher discharge capacity [2–4] and better large-current discharge ability [5,6], but also own the lower self-discharge rate [7].

RE–Mg–Ni-based hydrogen storage alloys are usually divided into  $\text{AB}_3$ - (CeNi<sub>3</sub>- and  $\text{PuNi}_3$ -),  $\text{A}_2\text{B}_7$ - ( $\text{Gd}_2\text{Co}_7$ - and  $\text{Ce}_2\text{Ni}_7$ -) and  $\text{A}_5\text{B}_{19}$ - ( $\text{Pr}_5\text{Co}_{19}$ - and  $\text{Ce}_5\text{Co}_{19}$ -) type phases according to different stacking

\* Corresponding author. State Key Laboratory of Metastable Materials Science and Technology, Yanshan University, Qinhuangdao 066004, PR China.

E-mail address: [hanshm@ysu.edu.cn](mailto:hanshm@ysu.edu.cn) (S. Han).

<sup>1</sup> These authors contributed equally to this work.

proportions of  $[\text{RENi}_5]/[\text{REMgNi}_4]$  subunit [8,9]. It is because of the special superlattice structures that RE–Mg–Ni-based alloys exhibit good electrochemical performance. Recent years, most studies have focused on La–Mg–Ni-based alloys, but the poor cycling stability limit their practical applications [10–12]. In this case, Nd–Mg–Ni-based hydrogen storage alloys with better cycling stability and high rate dischargeability (HRD) have attracted much attention [13,14]. Our previous study showed that, compared with the  $\text{PuNi}_3$ -type  $\text{La}_2\text{MgNi}_9$  alloy,  $\text{Nd}_2\text{MgNi}_9$  alloy exhibited a better cycling stability with a capacity retention rate of 92% after 100 charge/discharge cycles, and the HRD was 10% higher than that of  $\text{La}_2\text{MgNi}_9$  alloy at the discharge current density of  $1440 \text{ mA g}^{-1}$  [15]. Furthermore, it was found that Nd–Mg–Ni-based alloys had lower self-discharge rate and been successfully used as the negative materials of Ni/MH batteries with low self-discharge rate in Japan [16]. However, there is a lack of the theoretical research on the self-discharge characteristic of the Nd–Mg–Ni-based alloys.

Theoretically speaking, the self-discharge behaviors of alloy electrodes can be ascribed to two reasons [17], one is the desorption of hydrogen atoms from the hydride electrodes, named reversible self-discharge, and this part of capacity can be recovered by recharging it; the other is the oxidation/corrosion of active materials of alloy electrodes in the alkaline electrolyte, called irreversible self-discharge, and this part of capacity cannot be recovered. A study on the effect of different Ni contents on the self-discharge property of  $\text{Nd}_{0.88}\text{Mg}_{0.12}\text{Ni}_{3.10+x}\text{Al}_{0.20}$  ( $x = 0.00, 0.10, 0.20, 0.30$ ) alloys showed that, it was because of the lowest value of reversible and irreversible self-discharge when  $x = 0.20$  that the alloy electrode exhibited the best charge retention rate [18]. And in that study, different contents of Ni also generated the changes in phase structure of the alloys, while the influence of phase structures on the self-discharge rate was not mentioned. Young et al. studied the effect of various annealing conditions on the properties of the  $(\text{Nd,Mg,Zr})(\text{Ni,Al,Co})_{3.74}$  alloys [19]. They found that when the annealing treatment intensified, the as-cast alloy consisting of  $\text{ZrO}_2$ ,  $\text{A}_2\text{B}_7$  and  $\text{AB}_5$ -type phases gradually transformed into a single-phase  $\text{A}_2\text{B}_7$ -type alloy, leading to constant decrease of the self-discharge rate of the alloy electrodes, and the single-phase alloy had the lowest self-discharge rate. It is obvious that phase structure has important effect on the self-discharge rate of the alloys and alloys with single-phase structures have lower self-discharge rate. In fact, self-discharge characteristic of Nd–Mg–Ni-based hydrogen storage alloys with different single-phase structures is not clear and the self-discharge mechanism need to be further revealed.

In this work, single-phase  $\text{PuNi}_3$ ,  $\text{Gd}_2\text{Co}_7$ , and  $\text{Pr}_5\text{Co}_{19}$ -type Nd–Mg–Ni-based hydrogen storage alloys with  $[\text{NdNi}_5]/[\text{NdMgNi}_4]$  subunit ratios of 1:1, 2:1 and 3:1 have been prepared by a stepwise powder sintering method, respectively. Then the self-discharge characteristic and mechanism of the alloys have been systematically studied.

## 2. Experiments

Single-phase  $\text{Nd}_{0.8}\text{Mg}_{0.2}\text{Ni}_{3.0}$ ,  $\text{Nd}_{0.8}\text{Mg}_{0.2}\text{Ni}_{3.5}$  and  $\text{Nd}_{0.8}\text{Mg}_{0.2}\text{Ni}_{3.8}$  alloys were obtained by a stepwise sintering method using different precursors. Specifically,  $\text{Nd}_{0.8}\text{Mg}_{0.2}\text{Ni}_{3.0}$  and  $\text{Nd}_{0.8}\text{Mg}_{0.2}\text{Ni}_{3.5}$  alloys were prepared by  $\text{NdNi}$  and  $\text{MgNi}_2$  precursors, and  $\text{Nd}_{0.8}\text{Mg}_{0.2}\text{Ni}_{3.8}$  alloy was got using  $\text{Nd}_{0.8}\text{Mg}_{0.2}\text{Ni}_{2.7}$  and  $\text{Mg}_2\text{Ni}$  precursors. The precursors mentioned above were synthesized through inductive melting constituent elements under an Ar atmosphere. When preparing the sintered samples, the precursors were mechanically crushed firstly, ground into powder and passed the griddle of 300 meshes, then the precursor powders with certain ratios were blended for 3 min to guarantee the uniformity. After that, each mixture was cold pressed under the pressure of 10 MPa into a table of 3 g which was then wrapped by a nickel shell with fixed dimension to ensure the same volatilization of Mg in the sintering process. Finally, the samples were sintered in a tube furnace with the temperature rising from room

**Table 1**

Chemical composition of the three single-phase Nd–Mg–Ni-based alloys obtained by ICP.

Designed composition	Nd (wt.%)	Mg (wt.%)	Ni (wt.%)	Chemical composition
$\text{Nd}_{0.8}\text{Mg}_{0.2}\text{Ni}_{3.0}$	40.02	1.64	58.34	$\text{Nd}_{0.80}\text{Mg}_{0.20}\text{Ni}_{2.89}$
$\text{Nd}_{0.8}\text{Mg}_{0.2}\text{Ni}_{3.5}$	35.24	1.49	63.27	$\text{Nd}_{0.80}\text{Mg}_{0.20}\text{Ni}_{3.53}$
$\text{Nd}_{0.8}\text{Mg}_{0.2}\text{Ni}_{3.8}$	34.14	1.35	64.51	$\text{Nd}_{0.81}\text{Mg}_{0.19}\text{Ni}_{3.76}$

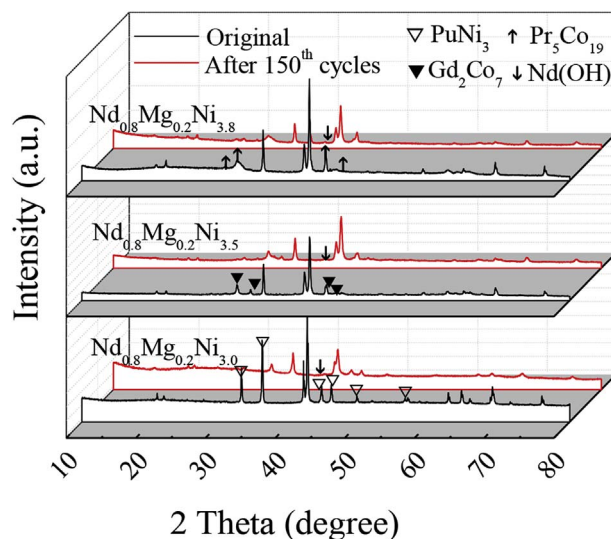


**Fig. 1.** XRD patterns of the original single-phase  $\text{Nd}_{0.8}\text{Mg}_{0.2}\text{Ni}_{3.0}$ ,  $\text{Nd}_{0.8}\text{Mg}_{0.2}\text{Ni}_{3.5}$  and  $\text{Nd}_{0.8}\text{Mg}_{0.2}\text{Ni}_{3.8}$  alloys and alloys after charging/discharging for 150 cycles in the  $2\theta$  range of  $10\text{--}80^\circ$ .

temperature to 1223 K, at which the samples were stayed warm for 4.5 d. During the period of raising temperature, three heat preservation stages were proceeded ( $873$ ,  $973$  and  $1073 \text{ K}$  holding 1 h at each temperature). When the sintering process finished, the samples were cooled down to room temperature together with the tube furnace. The chemical constitution of the final alloy samples were tested by the inductively coupled plasma (ICP) system and the test results were listed in Table 1. It is shown that the chemical compositions of the three single-phase alloys are in accordance with the designed compositions.

The alloys after sintering were ground into powder below 400 meshes to carry out X-ray diffraction (XRD) and selected area electron diffraction (SAED) measurements to determine their phase structures. XRD measurements were conducted with a D/Max-2500/PC X-ray diffractometer with  $\text{Cu K}\alpha$  radiation, and the XRD patterns were analyzed by Rietveld method using Rietica software. Then the accuracy of the refinement was judged by  $S$ , defined as  $R_{\text{wp}}/R_e$ , where  $R_{\text{wp}}$  is a residue of the weighted pattern and  $R_e$  is a statistically expectative residue.

For electrochemical tests, a three-electrode system composed of Ni  $(\text{OH})_2/\text{NiOOH}$  electrode as the counter electrode, Hg/HgO electrode as the reference electrode and the alloy electrode as the working electrode was used. To make the working electrode, 0.15 g alloy powder with 200–400 meshes together with 0.75 g carbonyl Ni powder was mixed uniformly. And the powder mixtures were cold pressed to pellets of 10 mm in diameter and 2 mm in thickness under 15 MPa, and then welded with nickel clavas. All the electrodes were put into the 6 M KOH solution steeping 24 h before tests. Then the battery systems were connected with the DC-5 battery testers. For activation, the systems were charged for 8 h and discharged with a current density of  $60 \text{ mA g}^{-1}$ , followed by charging at  $300 \text{ mA g}^{-1}$  for 1.6 h then discharging at  $60 \text{ mA g}^{-1}$  for cycling stability and self-discharge characteristic measurements. The self-discharge characteristic was explained by the charge retention rate (CRT), which was calculated by the following equality:

Download English Version:

<https://daneshyari.com/en/article/7726480>

Download Persian Version:

<https://daneshyari.com/article/7726480>

[Daneshyari.com](https://daneshyari.com)